Journal of Asian Ceramic Societies

ISSN: (Print) 2187-0764 (Online) Journal homepage: https://www.tandfonline.com/loi/tace20

Determination of optimum slurry evaluation method for the prediction of $BaTiO_3$ green sheet density

Naoya Iwata & Takamasa Mori

To cite this article: Naoya Iwata & Takamasa Mori (2020) Determination of optimum slurry evaluation method for the prediction of $BaTiO_3$ green sheet density, Journal of Asian Ceramic Societies, 8:1, 183-192, DOI: 10.1080/21870764.2020.1718859

To link to this article: https://doi.org/10.1080/21870764.2020.1718859

Published online: 28 Jan 2020.

JOURNAL OF ASIAN CERAMIC SOCIETIES
2020, VOL. 8, NO. 1, 183–192
https://doi.org/10.1080/21870764.2020.1718859

THE CERAMIC SOCIETY OF JAPAN
THE KOREAN CERAMIC SOCIETY
Taylor & Francis
Taylor & Francis Group

FULL LENGTH ARTICLE

Determination of optimum slurry evaluation method for the prediction of $BaTiO_3$ green sheet density

Naoya Iwata[a] and Takamasa Mori[b,c]

[a]Graduate School of Science and Engineering, Hosei University, Tokyo, Japan; [b]Department of Chemical Science and Technology, Faculty of Bioscience and Applied Chemistry, Hosei University, Tokyo, Japan; [c]Hosei University Research Institute for Slurry Engineering, Tokyo, Japan

ABSTRACT

In this study, the particle dispersion state in a dense $BaTiO_3$ slurry containing a dispersant and binder was assessed by various slurry evaluations such as particle size distribution measurement by laser diffraction, viscosity measurement, dynamic viscoelasticity measurement, and hydrostatic pressure measurement, which is a novel slurry evaluation technique developed by our group. Then, the relationship between the slurry evaluation results and the packing fraction of green sheets fabricated from these slurries was discussed. We found that the particle size distribution and the relative viscosity and yield stress by dynamic viscoelasticity measurement could not properly estimate the packing fraction of green sheets. In contrast, the hydrostatic pressure measurement was able to distinguish the particle dispersion state, and the results show an acceptable correlation with the packing fraction. The reason is that our developed method evaluates not only the initial particle dispersion state, but also its change as the particle concentration increases.

ARTICLE HISTORY
Received 13 September 2019
Accepted 17 January 2020

KEYWORDS
Slurry; particle dispersion state; tape casting; packing fraction; hydrostatic pressure measurement

1. Introduction

The ceramic wet-shaping process uses a slurry containing the base powder, medium, and several additives. The prepared slurry is turned into green body through the shaping and drying process. It is well known that the microstructure of the green body, which governs the product characteristics, is affected by the state of particle assembly in the slurry. Generally, a dense or sparse structure is obtained from a dispersed or aggregated slurry, respectively. Hence, the evaluation and control of particle dispersion state are very important for predicting the green body density in the manufacturing process [1–3]. For instance, Ryu et al. [1] investigated the effect of slurry pH on the dispersibility of aqueous alumina slurry and the properties of green and sintered bodies produced from tape casting. They concluded that an appropriate pH allows the particles to be well dispersed to produce a dense sintered body with homogeneous microstructure. Feng and Dogan [2] studied the effect of organic additives on the stability and rheological behavior of lanthanum-modified lead zirconate titanate slurry, as well as the strength and density of the corresponding green tapes. In that report, they determined the optimum amount of dispersant additive, which is important to characterize the particle dispersibility. Zhou et al. [3] used barium titanate slurry and also examined the optimum amount of dispersant for obtaining the highest densities in the green and sintered bodies.

Currently, several slurry evaluation techniques and apparatuses have been developed and adopted in research and industrial settings. Especially, there is increasing use of particle size distribution measurement based on the laser diffraction scattering method, and slurry flow property evaluation by using rheometer and rotational viscometer. In previous studies, however, there are instances when the results of such measurements do not correlate with the particle dispersibility in the slurry or the packing fraction of the green body. Particularly for the ceramic wet-shaping process, the slurry tends to have a high particle concentration and multicomponent additives such as binders; consequently, proper evaluation of its behavior is not easy [4–7]. For example, Singh et al. [4] investigated the colloidal stability of alumina suspensions and determined the optimum suspension pH. They demonstrated the effect of pH on the particle size distribution and sedimentation test results. However, the latter two properties were not completely correlated to each other, and there was no explanation for the mismatch. Yokoyama et al. [6] used a dense aqueous titanium nitride slurry containing 46.4 vol% of particles and studied the effect of dispersant condition on the slurry and green body characteristics. Those authors used rheological evaluations to confirm the slurry behavior and found that the green body density changed according to the dispersant type. Besides, they reported that the measured viscosity did not completely correlate with the density of green body; however, the cause was not clear. Davies and

CONTACT Naoya Iwata naoya.iwata.7d@stu.hosei.ac.jp 3–7–2 Kajino, Tokyo, Koganei 184–8584, Japan

Binner [7] also used a dense alumina slurry to experimentally investigate the rheological behavior and the density of a green body produced from these slurries containing different dispersant amounts. Although they found the optimum additive amount in terms of the rheological behavior and polymer configuration, the apparent viscosity of the slurry did not wholly correspond to the green body density for reasons that were not completely explained. Furthermore, dynamic viscoelasticity measurement has been used in recent years for evaluating the rheological characteristics of slurries [8–10]. Although this measurement is nondestructive and can give useful information, there are different interpretations of the measurement results, and therefore, it remains unknown whether the results correlate with the particle dispersion state and the density of the green body. In a previous study that conducted dynamic viscoelasticity measurement, Olhero and Ferreia [8] evaluated the dynamic properties of aluminum nitride slurry to investigate the critical shear stress, and then confirmed the presence of an internal structure. Nevertheless, the relationship between this result and the slurry and green body properties was not discussed. Komoda et al. [9] carried out strain and frequency sweep tests for a polymethylmethacrylate and graphite slurry to investigate the structural change during the particle dispersion process. Their results suggested that the particle dispersion state could be revealed using these tests; however, they did not compare the green body characteristics. Bitterlich et al. [10] performed dynamic measurement to characterize changes in the internal structure of the slurry with time and determine the strength of that internal network. After comparing the result with the green body measurements, they concluded that the highest density of the green body was obtained from the slurry having the weakest internal structure. Nevertheless, the two properties did not completely correlate, and more work was needed to use this evaluation.

On the other hand, our group has developed a hydrostatic pressure measurement method based on the particle sedimentation phenomenon. This method can distinguish the difference in sedimentation rate that depends on the particle dispersion state. It has also been used to effectively measure dense slurries directly [11–18]. However, it was not confirmed whether the results are correlated with the green body density.

Therefore, in this study various slurry evaluation methods were applied to slurries that were dense and contained multicomponent additives, and the obtained results were compared. Then, we investigated whether the results correspond to the packing fraction of green sheets fabricated from the same slurries.

2. Experimental procedures

2.1. Slurry preparation

Slurries were prepared from barium titanate powder (HPBT-1, Fuji Titanium Industry Co., Ltd.) with a density of 6.0 g·cm^{-3}, distilled water, polycarboxylic ammonium (PCA; Ceruna D-305, Chukyo Yushi Co., Ltd.) as a dispersant, polyvinyl alcohol (PVA; FUJIFILM Wako Pure Chemical Corporation) as a binder, and Nopco 267-A (San Nopco Ltd.) as a defoamer. The particle concentration was 45 vol%, the PCA dosage was 2–10 mg·g^{-1} for total particle mass, and the dosage of PVA and defoamer together was 0.3 mass% for total slurry mass.

First, a certain amount of PCA and distilled water were mixed under ultrasonication for 3 min, then the PCA solution and $BaTiO_3$ powder were mixed in a ball mill using zirconia balls (600 g, average size 4 mm). After 23 h, the PVA solution and defoamer were added, and ball-milling was conducted again for 1 h. Subsequently, the prepared slurry was degassed in vacuum for 5 min before use in the experiments. Each prepared slurry was 300 mL in volume.

2.2. Slurry evaluations

2.2.1. Particle size distribution measurement by laser diffraction method

The particle size distribution in the slurry was investigated by a laser diffraction particle size analyzer (SALD-2300, Shimadzu Corporation). To reduce the particle density to within the measurable range, the slurry was diluted by 50,000 times with distilled water, and stirred at 300 rpm using a magnetic stirrer. Particle size distribution of the raw powder was also measured. Figure 1 shows the pH dependency of zeta-potential for $BaTiO_3$

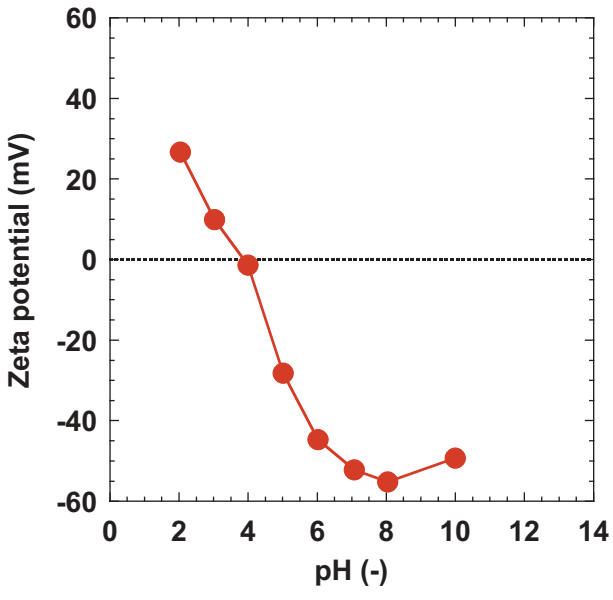

Figure 1. Zeta potential of $BaTiO_3$ particles as a function of pH.

particle measured by a zeta-potential analyzer (Model 502, Nihon Rufuto Co., Ltd.), confirming that the potential increased with increasing the pH. Therefore, an exceedingly low particle concentration of 1.0×10^{-5} vol% was obtained using the ultrasonic homogenizer, and its pH was adjusted at 10.4 using sodium hydroxide solution to prepare a dispersed thin slurry with a high potential of 50 mV. The measurement result was used as the primary particle diameter for this slurry.

2.2.2. Rheological characteristics evaluation

The flow curves of the prepared slurry were measured by a coaxial double-cylinder rotational viscometer (Rheolab QC, Anton Paar) with the shear rate changed from 0 to 200 s^{-1} and from 200 to 0 s^{-1} for 360 s. Moreover, strain sweep test was also conducted by using a viscoelasticity measurement apparatus (MCR 302, Anton Paar) with the amplitude from 10^{-5} to 10^{-1}% at a constant frequency of 1 Hz. Then, the shear stress, storage modulus (G'), and loss modulus (G'') of the slurry were investigated.

2.2.3. Hydrostatic pressure measurement

The hydrostatic pressure change with time at the bottom of cylinder containing the prepared slurry was measured by a hydrostatic pressure measurement apparatus (HYSTAP, JHGS Co., Ltd., Figure 2). Immediately after placing the slurry, the maximum hydrostatic pressure (P_{max}) is obtained since all the particles are suspended in the medium. As the particles settle and sediment, the hydrostatic pressure gradually decreases, reaching a minimum value (P_{min}) when all the particles are in the sediment as mentioned by Tsubaki et al. [11]. Since the settling and sedimentation rate depends on the particle size in the slurry, the particle assembly state can be distinguished by examining the decreasing slope of the hydrostatic pressure vs. time plot, as shown on the right side of Figure 2. The prepared slurry was put into an acrylic cylinder with an inner diameter of 40 mm, and the tip of transmission tube was fixed at the position of 10 mm from the bottom of the cylinder. P_{max} and P_{min} could be calculated theoretically by using the following equations:

$$P_{max} = \{\rho_l + \phi_0(\rho_p - \rho_l)\}g(H - 0.01) \quad (1)$$

$$P_{min} = \rho_l g(H - 0.01) \quad (2)$$

where ρ_l is the medium density ($kg \cdot m^{-3}$), ρ_p is the particle density ($kg \cdot m^{-3}$), g is the gravitational acceleration ($m \cdot s^{-2}$), ϕ_0 is the initial particle volumetric fraction (dimensionless), and H is the slurry height (m). The initial slurry height was 110 mm.

2.3. Tape casting

The slurries prepared in Section 2.1 were cast onto a stationary carrier film with a doctor blade setting at a height of 0.5 mm and a width of 150 mm. The casting speed was 0.6 $m \cdot min^{-1}$ over a length of 300 mm. The fabricated tapes were dried under room temperature to produce the green sheets. After calcining four pieces of the green sheet for each condition, their packing fractions were investigated by Archimedes' method.

3. Results

3.1. Slurry evaluations

3.1.1. Particle size distribution measured by the laser diffraction method

The particle size distribution measured by the laser diffraction particle size analyzer is shown in Figure 3. The particle size distributions of the different slurries are almost the same as the primary particle size distribution regardless of the PCA additive dosage. Therefore, the particles in these slurries were highly dispersed for all PCA dosages.

3.1.2. Rheological characteristics evaluation

The flow curves of the prepared $BaTiO_3$ slurry are shown in Figure 4. These slurries were non-Newtonian fluids since the curves are non-linear. Then, the apparent viscosities at a shear rate of 20 s^{-1} calculated from Figure 4 are shown in Figure 5. From this figure, it was found that the slurry with 2 $mg \cdot g^{-1}$ PCA had the lowest apparent viscosity, while that with 6 $mg \cdot g^{-1}$ PCA had the highest. As mentioned in the previous study [19], it was already

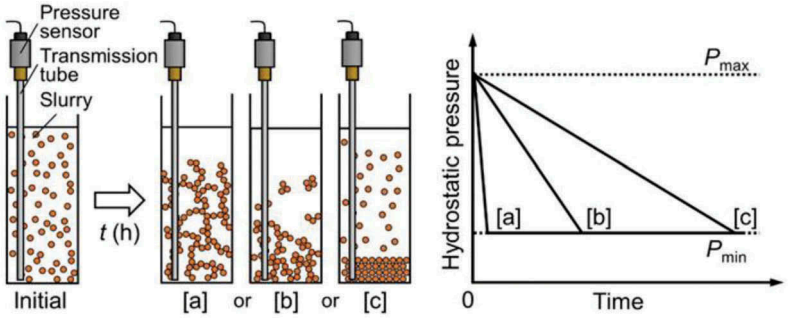

Figure 2. Schematic of hydrostatic pressure measurement and the different particle dispersion states: [a] gelation, [b] aggregation, [c] dispersion.

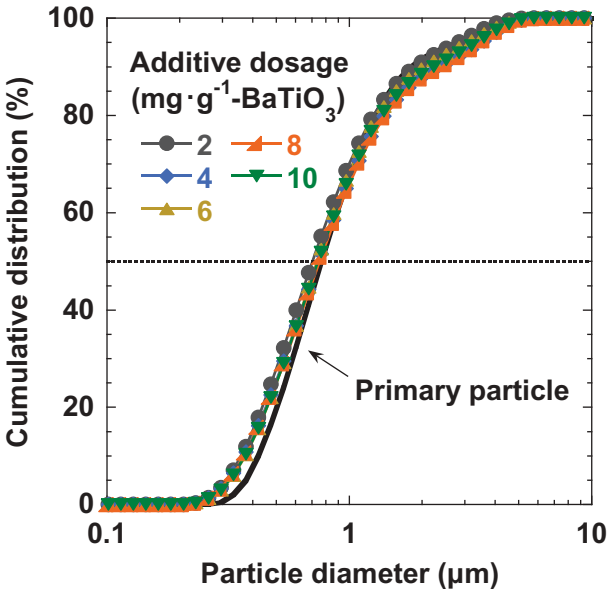

Figure 3. Cumulative distribution of $BaTiO_3$ slurry with various PCA additive dosages.

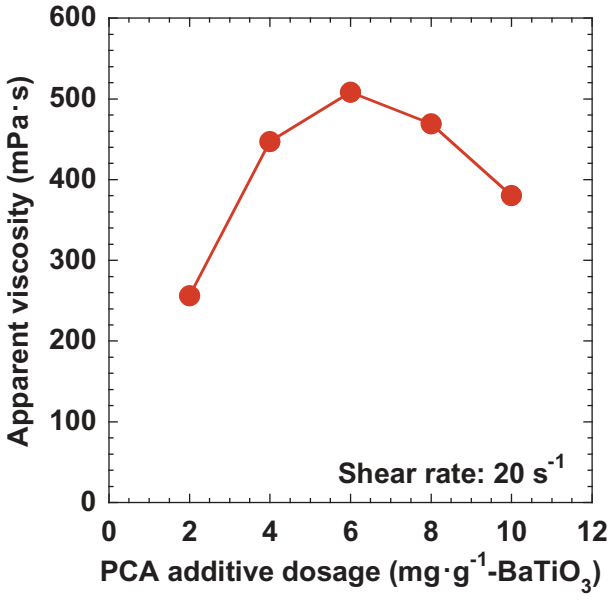

Figure 5. Apparent viscosity of $BaTiO_3$ slurry at a shear rate of 20 s^{-1} as a function of PCA additive dosage.

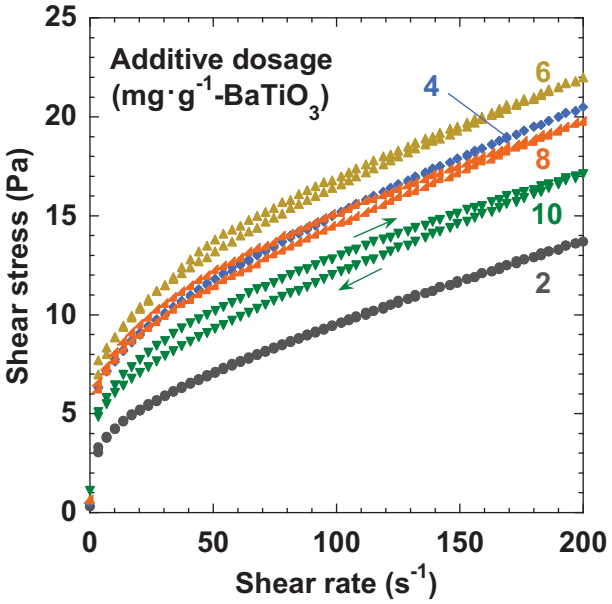

Figure 4. Flow curves of $BaTiO_3$ slurry with various PCA additive dosages.

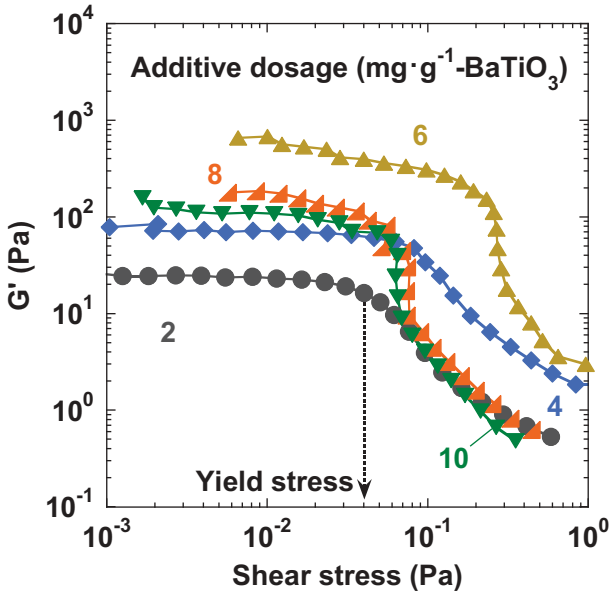

Figure 6. Storage modulus as a function of shear stress of $BaTiO_3$ slurry with various PCA additive dosages.

confirmed that this apparent viscosity change with PCA additive dosage was occurred by changing particle dispersion state and viscosity of medium. Therefore, it was found that the PCA 2 mg·g^{-1} added slurry was most dispersed within the range of these PCA additive dosages from this result.

The result of strain sweep test by dynamic viscoelasticity measurement is given in Figure 6, showing the storage modulus (G') which represents the elastic portion of viscoelastic body as a function of shear stress. In the actual measurement, although the loss modulus (G'') representing its viscus portion was also measured, these plots were omitted to make the difference of G' clear. At low shear stress, it was confirmed that the elastic behavior was dominant since $G' > G''$ for any PCA dosage and these moduli remained nearly constant. This result indicates that a microstructure was formed by the particles or binder. As the shear stress increased, G' suddenly decreased and crossed G''. At this point, the microstructures were broken down at the yield stress, and then these slurries began to behave like a fluid. Therefore, the yield stresses for each PCA additive dosage are taken from Figure 6 as shown in it, and then the variation depending on PCA additive dosage is shown in Figure 7. As can be seen from this figure, the yield stress variation had a similar

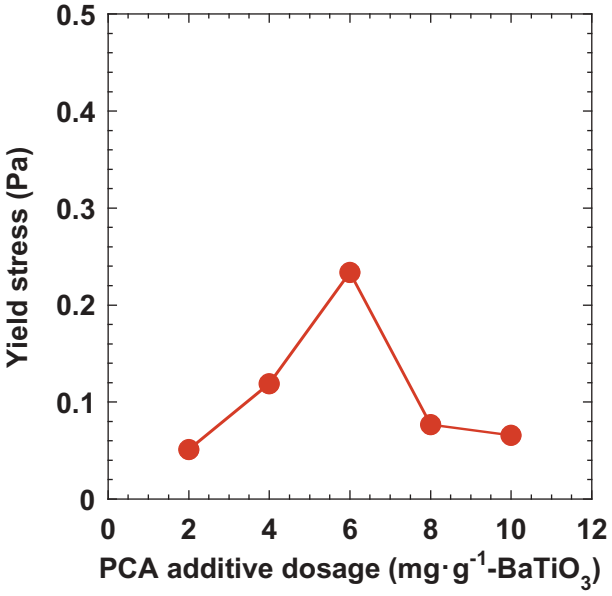

Figure 7. Yield stress of $BaTiO_3$ slurry as a function of PCA additive dosage.

trend with Figure 5; hence, this behavior may be caused by changing of particle dispersion state and rheological characteristic of the medium.

3.1.3. Hydrostatic pressure measurement

Figure 8 shows the measurement result of hydrostatic pressure in the slurry. From this figure, it was found that these results had large fluctuation and became hard to show the difference of slurry with each PCA additive dosage; however, it was reasonably considered to take the bottom of fluctuation because the hydrostatic pressure decreases by particle depositing in this method as shown in Figure 9. Consequently, it can be recognized that the negative slopes of hydrostatic pressure changed according to the PCA dosage, in particular, the

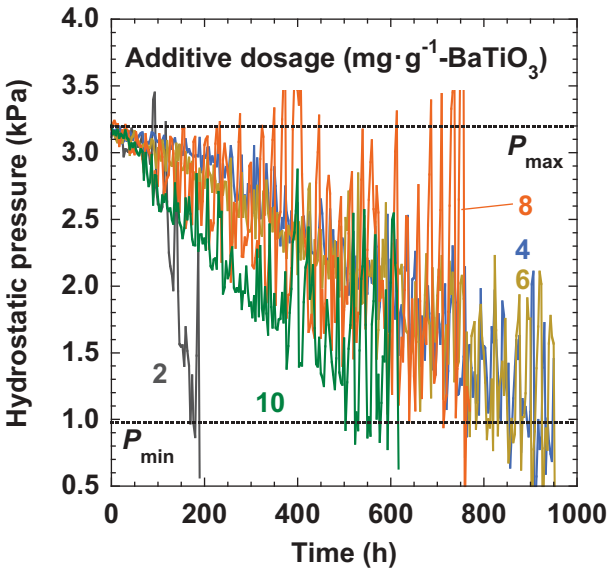

Figure 8. Hydrostatic pressure curves of $BaTiO_3$ slurry with various PCA additive dosages.

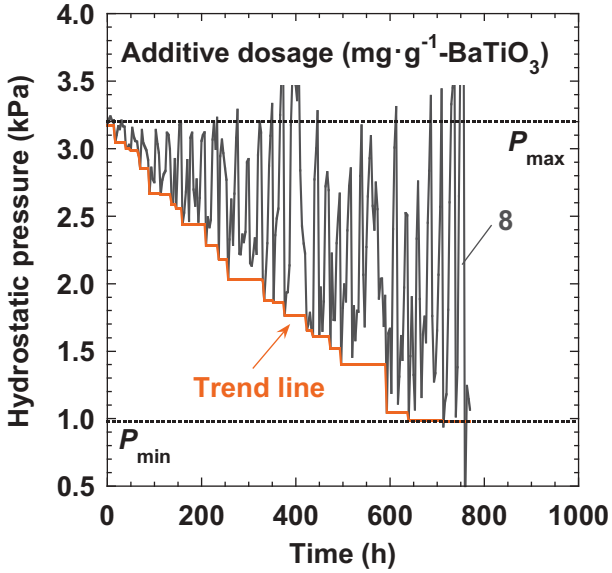

Figure 9. Trend line of measurement hydrostatic pressure curve of PCA 8 $mg \cdot g^{-1}$ added slurry.

slopes were the smallest for the slurries with 4 and 6 $mg \cdot g^{-1}$ PCA, which means that these particles were well dispersed. On the other hand, the slope of the slurry with 2 $mg \cdot g^{-1}$ PCA changed drastically 100 h after the start of measurement. It is considered that the particles flocculated and formed gelation structure due to the sedimentation concentration at that point, after maintaining the same dispersion state from the beginning. The same phenomena were confirmed in previous works [11–13,16–18]

3.2. Properties of green sheets

The measured packing fractions of the green sheets are shown in Figure 10. The bars in this figure indicate

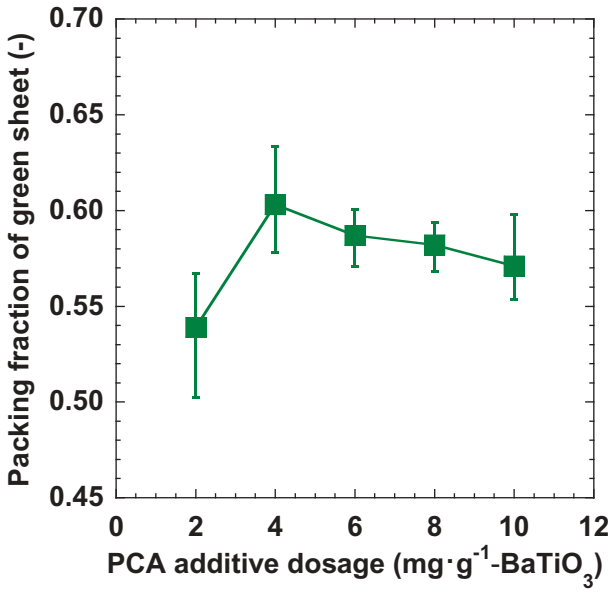

Figure 10. Effect of PCA additive dosage on the packing fraction of green sheet.

the maximum and minimum values. The slurry with 4 mg·g^{-1} PCA produced the highest packing fraction of 0.63, whereas that with 2 mg·g^{-1} PCA had the lowest packing fraction of 0.54. Figure 11 shows the image of the green sheet surface observed by a scanning electron microscope. The white arrows indicate the pore. From these pictures, the green sheets obtained with 2 and 10 mg·g^{-1} PCA added into the slurry had some large pores, while those with 4 and 6 mg·g^{-1} PCA were homogeneously and densely packed. Hence, the particle dispersion state changed with the PCA additive dosage.

4. Discussion

4.1. Correlation between slurry evaluation results and packing fraction of green sheet

Figure 12 shows the relationship between the median diameter measured by laser diffraction scattering method and packing fraction of green sheet. The bars in this figure indicate standard deviation. In this figure, there is no correlation between the median diameter and packing fraction of green sheet. In particular, the median diameter of particles in the slurries with 2 and 10 mg·g^{-1} PCA (considered to be aggregated particles from Figure 10) was equal to that of 4 mg·g^{-1} PCA, while the corresponding green sheets have significantly different packing fractions. Therefore, this method could not properly evaluate the particle dispersion state in the slurry. This may be caused by the dilution operation, since the obtained median diameters for all PCA dosages correspond reasonably well with the primary particle size of 0.79 μm. In other words, even if these particles were aggregated in the original slurry, the aggregates were not strong enough and disintegrated following 50,000 times dilution and stirring at 300 rpm. Additionally, the dilution dramatically decreased the particle concentration and enlarged the inter-particle distance, and the resultant low collision frequency prevented the re-formation of aggregates.

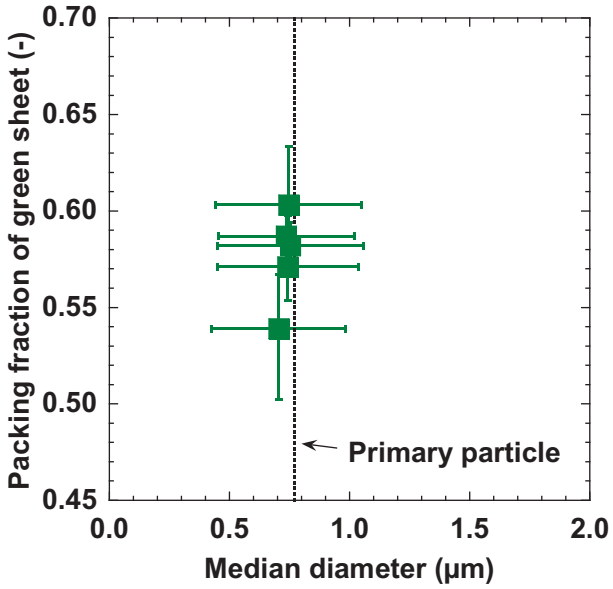

Figure 12. Relationship between median diameter measured by laser diffraction scattering method and packing fraction of green sheet.

Table 1 shows the apparent viscosity at the shear rate of 20 s^{-1} for the slurries in Figure 4, and the viscosity of the respective medium containing PCA, PVA, defoamer, and deionized water but no $BaTiO_3$ particles. Generally, only the apparent viscosity is commonly used for distinguishing the particle dispersion state in flow property characterization. In past studies, Song et al. [20], Jean and Wang [21], and Jin et al. [22] optimized the particle dispersion state by using the apparent viscosity for barium titanate and yttria slurries, respectively. However, Table 1 confirms that the viscosity of the medium changed with the PCA dosage. To take this into account, the result was analyzed in terms of relative viscosity (the ratio of the slurry viscosity to that of medium), which is an effective way to compare the particle dispersion state when the viscosity of medium changes. In their previous works, Nagata [23] and Nagata and Takase [24] adopted the relative viscosity for comparing the particle dispersion state of alumina slurries. Smay and Lewis [25] performed a similar analysis

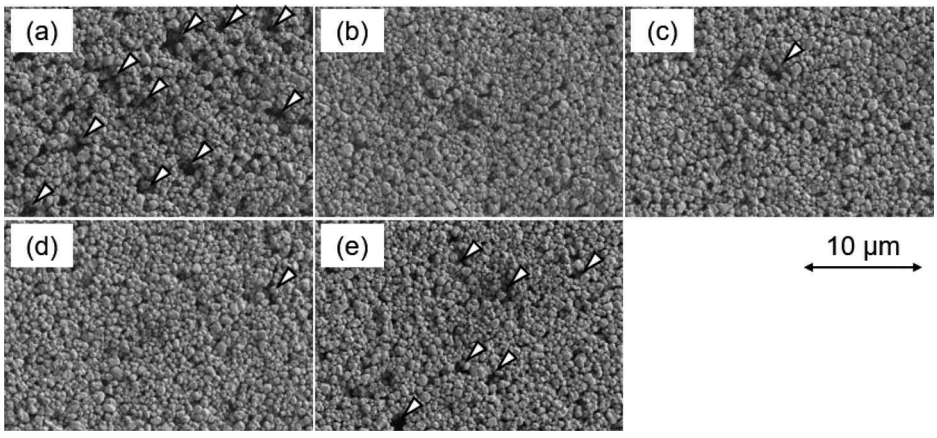

Figure 11. SEM photos of $BaTiO_3$ green sheet surface with various PCA additive dosages: (a) 2, (b) 4, (c) 6, (d) 8, and (e) 10 mg·g^{-1}.

Table 1. Apparent viscosities of $BaTiO_3$ slurries and the medium with various PCA additive amounts.

PCA additive dosage ($mg \cdot g^{-1}$)	2	4	6	8	10
Apparent viscosity of slurry at a shear rate of 20 s^{-1} ($mPa \cdot s$)	256	447	508	469	380
Viscosity of medium, μ_s ($mPa \cdot s$)	4.38	3.72	3.24	3.74	3.10

for lead zirconate titanate slurries, taking into account the different viscosity of the medium. Comparison between the packing fraction of green sheet and the calculated relative viscosity is shown in Figure 13. It is thought that the relative viscosity decreases when particles in a slurry are dispersed, and then the packing fraction of green sheet should increase. However, Figure 13 shows the reverse correlation. In particular, the green sheet with the lowest packing fraction was obtained from the slurry with 2 $mg \cdot g^{-1}$ added PCA, which had the lowest relative viscosity of 58.5. Hence, the viscosity measurement could not correctly predict the packing fraction of green sheet.

Next, we compare the slurry properties evaluated by dynamic viscoelasticity measurement and the packing fraction of green sheet. As it previously mentioned in the introduction, Bitterlich et al. [10] had concluded that the densest green body was obtained from a slurry with the lowest yield stress as measured by strain sweep test. Therefore, we investigated whether the packing fractions were correlated with the yield stress in this study. From the results in Figure 14, there is no such correlation, as the lowest packing fraction corresponded to the lowest yield stress of 0.05 Pa, being the opposite of previous work. Hence, this method could not properly estimate the particle dispersion state in this study.

Regarding the hydrostatic pressure measurement, since the sedimentation rate is dependent on the particle dispersion state, the time corresponding to P_{min} is denoted as t^* (h), and its measured values are 182, 930, 817, 623, and 495 h for the PCA contents of 2, 4, 6, 8, and 10 $mg \cdot g^{-1}$, respectively. These t^* values were used for comparison with the packing fraction of green sheets. Besides, the medium viscosity differs according to the PCA dosage (Table 1). In general, the particle settling velocity is in inverse proportion to the viscosity of the medium (μ_s). Thus, t^*/μ_s (Pa^{-1}) was used as the dispersion index and compared to the packing fraction of green sheet (Figure 15). In this figure, the packing fraction of green sheet increases with increasing t^*/μ_s.

According to the above results, the hydrostatic pressure measurement could distinguish the particle dispersion state more precisely than other slurry evaluation

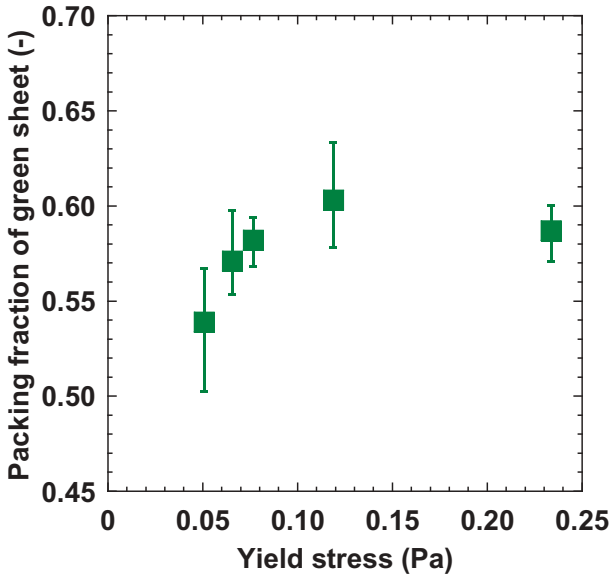

Figure 14. Relationship between yield stress measured by strain sweep test and packing fraction of green sheet.

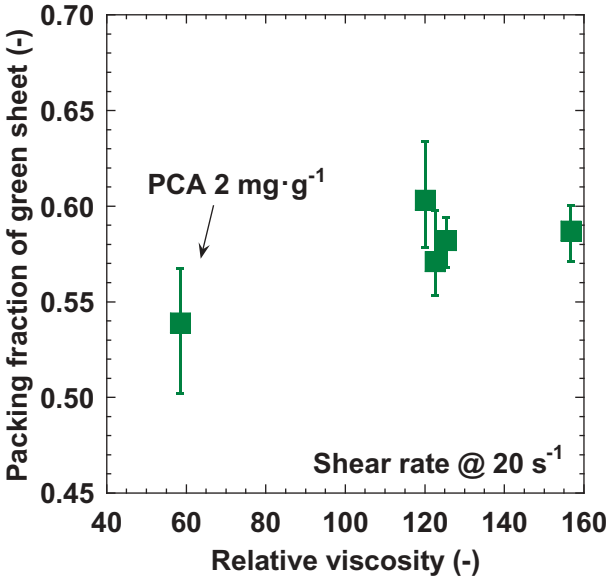

Figure 13. Relationship between relative viscosity at a shear rate of 20 s^{-1} and packing fraction of green sheet.

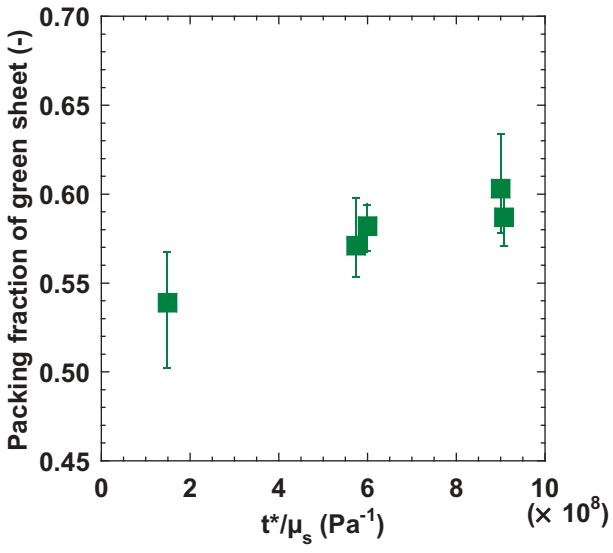

Figure 15. Relationship between t^*/μ_s and packing fraction of green sheet.

methods, as well as estimate the packing fraction of green sheet fabricated from the slurry.

4.2. Difference between hydrostatic pressure measurement and viscosity measurement

Now, why is the packing fraction of green sheet correlated with the hydrostatic pressure measurement result, instead of that from the rheological evaluation (especially the relative viscosity of slurry)? In Figure 13, the correlation between the packing fraction and relative viscosity was poor, especially that the slurry with 2 mg·g^{-1} added PCA did not fit the trend. In previous works, Tsubaki et al. [11], Mori et al. [12,16] and Ohtsuka et al. [26] gave some examples when the apparent viscosity of a slurry does not correspond to the result of gravitational sedimentation test, and observed the phenomenon of time-dependent viscosity change in an alumina slurry due to change in the particle dispersion state. Furthermore, Hotta et al. [27] also reported that the change of particle dispersion state with time was caused by the degradation of the dispersant during the ball-milling process. These were explained in terms of the agglomeration mechanism due to insufficient repulsive force between particles, and the increasing particle collision frequency with time by sedimentation concentration or stirring. Hence, the same phenomenon is considered to have occurred in the slurry containing 2 mg·g^{-1} PCA in this study. When using hydrostatic pressure measurement in systems displaying the sedimentation process, comparing the hydrostatic pressure change could distinguish the transition of particle assembly state. On the other hand, the green sheet was fabricated from the slurry through a drying process, in which particle concentration similarly occurred. In other words, the hydrostatic pressure measurement, which can show the transition of particle assembly state caused by sedimentation concentration, is more suitable for estimating the packing fraction of green sheet than the viscosity measurement in which the particle concentration is not changed. However, the product of the initial slope of hydrostatic pressure and the medium viscosity represents the particle dispersion state immediately after the preparation (before aging), so this value is expected to correlate to the relative viscosity of the slurry. Then, the initial slope denoted as m_i (Pa·h^{-1}) is obtained from Figure 8, and a comparison between its value multiplied by the medium viscosity, $m_i \cdot \mu_s$ (Pa^2) and the relative viscosity of slurry are shown in Figure 16. Consequently, a full correlation between $m_i \cdot \mu_s$ and the relative viscosity was confirmed. Moreover, after one full measurement, the sediments were broken by the stirring rod, and then the flow curves were measured again (Figures 17 and 18). From Figures 4, 17, and 18, it was found that the flow curves of slurries with 4, 6, 8, and 10 mg·g^{-1} added PCA showed almost no change with time owing to the sufficient repulsion force, whereas that apparent viscosity with 2 mg·g^{-1} PCA was significantly increased at any shear rate. Thus, the change of particle dispersion state was also confirmed in this method.

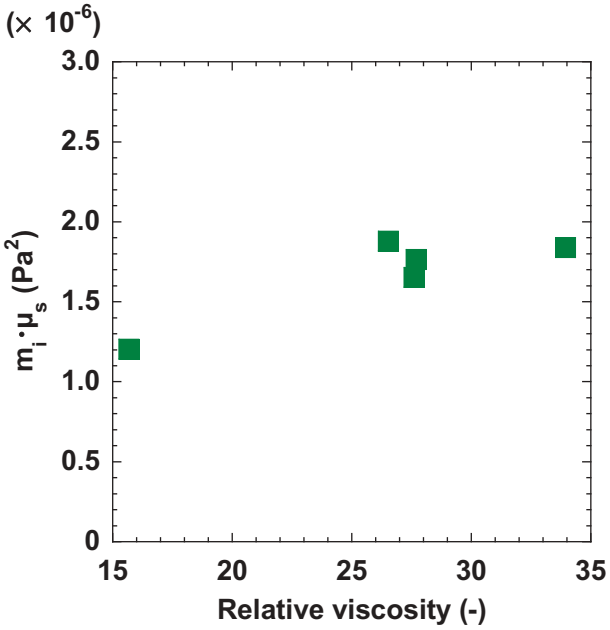

Figure 16. Relationship between relative viscosity at a shear rate of 20 s^{-1} and $m_i \cdot \mu_s$.

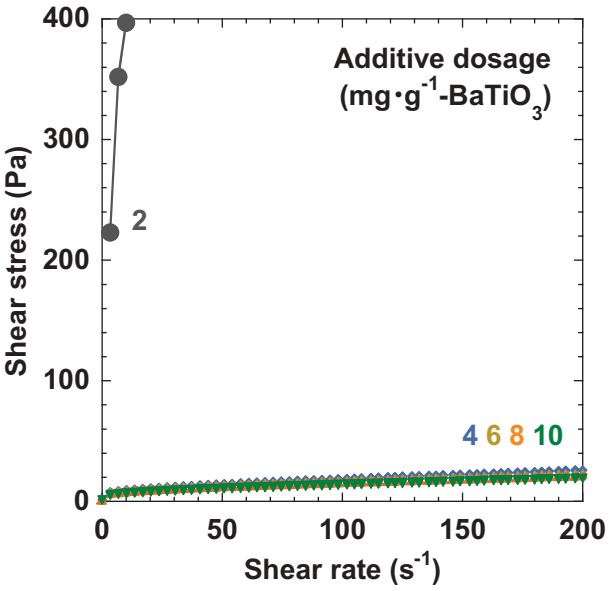

Figure 17. Flow curves of $BaTiO_3$ slurry after sedimentation and stirring.

The result of dynamic viscoelasticity measurement is considered to be similar to the viscosity, namely, the main cause for decrease in the packing fraction of green sheet could not be determined, since the slurry with 2 mg·g^{-1} added PCA showed no gelation immediately after preparation. While the viscosity and dynamic viscoelasticity measurements differ from each other by being destructive or not,

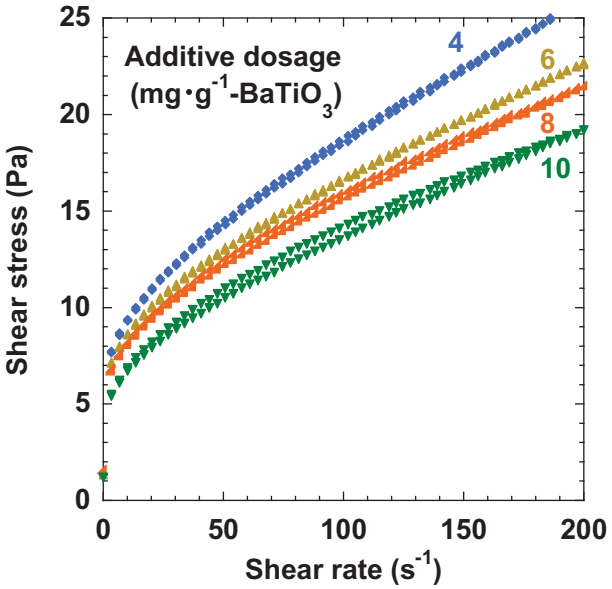

Figure 18. Enlarged bottom part of Figure 17.

however, neither includes a concentration process. As a result, we found that these evaluation methods could not properly predict the packing fraction of green sheet.

From the above, it was shown that the hydrostatic pressure measurement is a valid technique for predicting the packing fraction of green body fabricated by tape casting, because such measurement includes the particle concentration process.

5. Conclusion

The particle dispersion state of dense aqueous $BaTiO_3$ slurry was evaluated by various methods, and the results were compared with the packing fraction of green sheets fabricated from these slurries. The following results were obtained.

(1) The particle size distribution measurement by laser diffraction scattering method does not correspond to the packing fraction of green sheet, since the dilution prior to measurement affects the particle dispersion state in the slurry.
(2) Evaluation by viscosity and dynamic viscoelasticity measurements, especially the yield stress using strain sweep test, could not estimate the packing fraction of green sheet properly when the particle dispersion state of prepared slurry is changed by aging with sedimentation concentration.
(3) On the other hand, the value of t^*/μ_s obtained from hydrostatic pressure measurement is correlated with the packing fraction of green sheet, since this index takes into account the concentration process.

Acknowledgments

The authors acknowledge financial supports of the Adaptable and Seamless Technology Transfer Program (A-STEP) (JPMJTS1618) from Japan Science and Technology Agency (JST), and Hosokawa Powder Technology Foundation (18501).

Disclosure statement

No potential conflict of interest was reported by the authors.

Funding

This work was supported by the Adaptable and Seamless Technology Transfer Program through Target-Driven R and D [JPMJTS1618] from Japan Science and Technology Agency (JST); Hosokawa Powder Technology Foundation [18501].

ORCID

Naoya Iwata http://orcid.org/0000-0003-2312-2492

References

[1] Ryu B, Takahashi M, Suzuki S. Rheological characteristics of aqueous alumina slurry for tape casting. J Ceram Soc Jpn. 1993;101(6):643–648.
[2] Feng J, Dogan F. Aqueous processing and mechanical properties of PLZT green tapes. Mater Sci Eng A. 2000;283:56–64.
[3] Zhou D, Chen Y, Zhang D, et al. Fabrication and characterization of the multilayered PTCR ceramic thermistors by slip casting. Sens Actuators A. 2004;116:450–454.
[4] B P S, Menchaves R, Takai C, et al. Stability of dispersions of colloidal alumina particles in aqueous suspensions. J Colloid Interf Sci. 2005;291:181–186.
[5] Hirata Y, Nishimoto A, Ishihara Y. Effects of addition of polyacrylic ammonium on colloidal processing of α-alumina. J Ceram Soc Jpn. 1992;100(8):983–990.
[6] Yokoyama H, Kato N, Nomura T, et al. Effect of slurry characters of titanium nitride on forming and sintering behaviors. J Ceram Soc Jpn. 1999;107(10):968–972.
[7] Davies J. Binner J G P. The role of ammonium polyacrylate in dispersing concentrated alumina suspensions. J Eur Ceram Soc. 2000;20:1539–1553.
[8] S M O. Ferreia J M F. Rheological characterisation of water-based AlN slurries for the tape casting process. J Mater Process Technol. 2005;169:206–213.
[9] Komoda Y, Chizaki Y, Suzuki H, et al. Viscoelastic analysis of dispersion process of highly concentrated suspension for LiB cathodes. Journal of the Society of Powder Technology, Japan. 2016;53:371–379.
[10] Bitterlich B, Lutz C, Roosen A. Rheological characterization of water-based slurries for the tape casting process. Ceram Int. 2002;28:675–683.
[11] Tsubaki J, Kuno K, Inamine I, et al. Analysis of sedimentation and settling process of dense alumina slurries by hydrostatic pressure measurement. J Soc Powder Technol Jpn. 2003;40:432–437.
[12] Mori T, Ito M, Sugimoto T, et al. Slurry characterization by hydrostatic pressure measurement –effect of initial

height on sedimentation behavior–. J Soc Powder Technol Jpn. 2004;41:522–528.
[13] Mori T, Kuno K, Ito M, et al. Slurry characterization by hydrostatic pressure measurement –analysis based on apparent weight flux ratio. Adv Powder Technol. 2006;17:319–332.
[14] Mori T, Tsubaki J. Novel approach to characterization and control of fine particle suspensions. J Soc Powder Technol Jpn. 2008;45:835–843.
[15] Satone H, Nishiuma K, Iimura K, et al. Particle size measurement by hydrostatic pressure measurement method – effect of initial concentration. J Soc Powder Technol Jpn. 2011;48:456–463.
[16] Mori T, Kitagawa R. Experimental study on the time change in fluidity and particle dispersion state of alumina slurries with and without sintering aid. Ceram Int. 2017;43:13422–13429.
[17] Tanaka T, Asai K, Mori T, et al. Evaluation of particle assembling state in slurries for a cathode of Li-ion battery. J Soc Powder Technol Jpn. 2011;48:761–767.
[18] Iwata N, Mori T. Effects of particle dispersion on the properties of suspension-sprayed coatings. J Ceram Soc Jpn. 2017;125(10):783–788.
[19] Iwata N, Mori T. Effect of binder addition on optimum additive amount of dispersant for aqueous $BaTiO_3$ slurry. Ceram Int. 2019;45:19644–19649.
[20] Song Y, Liu X, Zhang J, et al. Rheological properties of nanosized barium titanate prepared by HGRP for aqueous tape casting. Powder Technol. 2005;155:26–32.
[21] Jean J, Wang H. Dispersion of aqueous barium titanate suspensions with ammonium salt of poly(methacrylic acid). J Am Ceram Soc. 1998;81(6):1589–1599.
[22] Jin L, Mao X, Wang S, et al. Optimization of the rheological properties of yttria suspensions. Ceram Int. 2009;35:925–927.
[23] Nagata K. Rheological behavior of suspension and properties of green sheet. J Ceram Soc Jpn. 1992;100:1271–1275.
[24] Nagata K, Takase H. Effect of molecular weights of polymers on rheological behavior of alumina suspension and properties of alumina green sheets. J Soc Powder Technol Jpn. 2007;44:574–580.
[25] J E S, Lewis JA. Structural and property evolution of aqueous-based lead zirconate titanate tape-cast layers. J Am Ceram Soc. 2001;84:2495–2500.
[26] Ohtsuka H, Mizutani H, Iio S, et al. Effects of sintering additives on dispersion properties of Al_2O_3 slurry containing polyacrylic acid dispersant. J Eur Ceram Soc. 2011;31:517–522.
[27] Hotta Y, Yilmaz H, Shirai T, et al. State of the dispersant and particle surface during wet-jet milling for preparation of a stable slurry. J Am Ceram Soc. 2008;91(4):1095–1101.